

1. AGENCY USE ONLY (Leave Blank)

Final Report

5. FUNDING NUMBERS
F49620-03-1-0275

6. AUTHOR(S)
Cammy R. Bernathy

8. PERFORMING ORGANIZATION
REPORT NUMBER final 1

Department of Air force, 4015 Wilson Blvd. Ropom 713
Arlington, VA 22203-1954

10. SPONSORING / MONITORING
AGENCY REPORT NUMBER

Final 1

The views, opinions and/or findings contained in this report are those of the author(s) and should not be construed as an official, AFOSR, policy or decision, unless so designated by other documentation.

12 b. DISTRIBUTION CODE

13. ABSTRACT (Maximum 200 words)

This award provided funding to purchase a new metal organic chemical vapor deposition (MOCVD) system for growth of GaN-based materials and devices. .

15. NUMBER OF PAGES

10

16. PRICE CODE

18. SECURITY CLASSIFICATION
ON THIS PAGE
UNCLASSIFIED

19. SECURITY CLASSIFICATION
OF ABSTRACT
UNCLASSIFIED

20. LIMITATION OF ABSTRACT

UL

III-Nitride Metalorganic Chemical Vapor Deposition System for Development of High Power Electronics

DEFENSE UNIVERSITY RESEARCH INSTRUMENTATION PROGRAM

Final Report

Submitted to:
U. S. Air Force Office of Scientific Research

Technical P.O.C: C. R. Abernathy
Department of Materials Science and Engineering
Rhines Hall
University of Florida
Gainesville, FL 32611
Tel: 352 392-0943
Fax: 352 392-9673
caber@ufl.edu

Administrative P.O.C: Angela Hunter-Edwards
Department of Materials Science and Engineering
University of Florida
Rhines Hall
Gainesville, FL 32611
Tel: 352 392-1218

20041230 027

1. Abstract

This award provided funding to purchase a new metal organic chemical vapor deposition (MOCVD) system for growth of GaN-based materials and devices. By combining the money provided by the DURIP award with donations from industry and matching funds from the University of Florida, an epitaxial facility worth ~\$1M has been constructed. This facility will be used to provide device structures for fabrication of high power GaN-based HEMTs and MOSFETs. This facility will benefit multiple DOD programs including two currently funded by the electronics programs at the U.S. Office of Naval Research (Development Of GaN MOSFETS And MISFETS, US Navy N00014-98-1-0204, Dr. Harry Dietrich) and the U. S. Air Force Office of Scientific Research (Development Of Passivation Technology For Improved GaN/AlGaN HEMT Performance And Reliability, U. S. Air Force F49620-02-1-0366, Dr. Gerald Witt). These contracts are aimed at developing improved dielectrics for high power GaN devices and to date have produced significant advances in the quality and effectiveness of dielectric/GaN interfaces. Because of this award, we can now capitalize on the successful oxide development generated by these programs. This equipment will provide a controlled in-house supply of GaN/AlGaN device material in order to identify much more precisely the role of a variety of material parameters as well as device layer structure in the performance of devices containing oxide/nitride interfaces. Acquisition of this system will also enable new avenues of investigation including resistance to thermal, electrical and radiation degradation for both all-nitride and nitride/oxide devices. Finally, acquisition of this MOCVD system will now allow development of a well controlled in-house device technology of the type needed to fabricate more advanced structures and prototypes including ultra-broadband high power and high dynamic range direct-conversion RF transmitters and high temperature III-nitride based gas sensors.

2. Technical Justification

Acquisition of the requested equipment will directly benefit two existing DOD contracts, Development Of Passivation Technology For Improved GaN/AlGaN HEMT Performance And Reliability U. S. Air Force F49620-02-1-0366 (P.I. C. R. Abernathy) and Development Of GaN MOSFETs And MISFETS US Navy N00014-98-1-0204 (P. I. C. R. Abernathy). Both contracts are directed toward improving the performance of GaN-based electronics through the development of improved dielectrics. AlGaIn/GaN high electron mobility transistors (HEMTs) show great promise for applications in which high speed and high temperature operation are required, such as high frequency wireless base stations and broad-band links, commercial and military radar and satellite communications[1-30]. These devices appear capable of producing very high power densities ($>12\text{W}\cdot\text{mm}^{-1}$), along with low noise figures (0.6dB at 10GHz) and high breakdown voltage. A number of recent reviews have appeared on this topic[31-35]. Developing these devices will provide the DOD with the next generation strategic technology. It should be noted that this is a true multiple-use technology, with direct application in hybrid drivetrain automobiles, next-generation battleships and submarines, the "more-electric" airplane, power transistors for communication power stations and in industrial machinery. However, while the concept of using wide bandgap semiconductors to structure power RF electronic devices has been discussed in the professional community over the last few years, several fundamental issues remain which must be addressed before technology insertion can be accomplished. Among other issues, one of the chief developments that must take place is in the area of improving the insulators that can be used in conjunction with the wide bandgap devices. Not only would development of a high quality GaN/oxide interface enable fabrication of an enhancement mode

(i.e. normally off) device, the use of metal-oxide-semiconductor (MOS) gates for GaN based MOSHEMTs produces a number of advantages over the more conventional Schottky metal gates, including lower leakage current and greater voltage swing[3,22,26,28-30]. Another area which can be addressed through development of dielectrics is a problem commonly observed in HEMT devices, the so-called "current collapse," in which the application of a high drain-source voltage leads to a decrease of the drain current and increase in the knee voltage[5,7,14-20,23]. This phenomenon can also be observed by a current dispersion between dc and pulsed test conditions, degraded rf output power and dispersions in transconductance and output resistance.

3. Description of the New GaN Epitaxial Facility

Funds provided by the AFOSR DURIP program in combination with funds provided by the University of Florida have been used to purchase a new Emcore (now VEECO) Pioneer 75 GaN metal organic chemical vapor deposition (MOCVD) system. The system is shown at the new UF MOCVD GaN facility in Figures 1 and 2. In exchange for a collaboration agreement with Veeco, the purchase price of this system was deeply discounted below the standard retail price. The PIONEER™ 75 Growth System includes the following:

EMCORE® water cooled PIONEER™ 75 FlowFlange® assembly with linear alkyl injection manifold, hydride injection manifold, hydrogen shroud flow manifold and pyrometer viewport.

PIONEER™ 75 Stainless steel growth chamber with:
front viewport w/ shutter; one loadlock pass-through w/ shutter.

Removable single zone resistive heater assembly with heat shields, electrical connectors and insulators.

Low differential MFC's for alkyl distribution, regulating valves for hydride distribution and hydrogen shroud distribution.

Needle valves for hydrogen purge of viewports, and loadlock pass-through.

Integrated magnetofluidic rotation mechanism, motor, and drive assembly.

EMCORE® TurboDisc® rotating shell susceptor for 75 mm wafer carriers, with integrated spindle.

Water cooled base plate assembly with electrical and thermocouple feedthrus and temperature regulation.

PIONEER™ 75 Growth Pump System with 1.5" exhaust line. This subsystem includes:

- Manual ball valve.
- Disposable particle filter.
- Pneumatic ball valve.
- KF-40 leak detector port.
- Electronic pressure transducer.

Throttling gate valve.

Rotary vane pump with overpressure protection, recirculating oil filter, oil coalescing filter, and auto ballast control valve, Electronic indicator system.

Krytox oil charge.

Molecular sieve filter.

Epimetric Insitu Monitor with a Single Head (EPI/1) System which enables Absolute Growth Rate Measurement and Real-time process stability verification.

Sekidenko One-sensor Pyrometer Single color optical fiber temperature measurement system. □

PIONEER™ 75 Loadlock System which includes:

PIONEER™ 75 stainless steel loadlock for 75 mm wafer carriers, with pass through flange, quick access loading door with interlocked latch, and two viewports.

PIONEER™ 75 Platter Transfer System. with a linear transfer fork with magnetically coupled manual control system and three high purity 75 mm wafer carriers plus one (1) blank carrier for temperature calibration.

Pneumatic gate valve.

Toxic gas sampling port.

PIONEER™ 75 Loadlock Pump system

EMCORE® Beam Splitter which allows installation of Epimetric or Epimetric II in combination with a Sekidenko Pyrometer on a single viewport.

EMCORE® PIONEER™ Gas Panel Sub Assembly which includes:

Integrated injection gas manifolds.

Metal sealed mass flow controllers for gas distribution.

Electronic pressure measurement.

Fast switching pneumatic valves for gas distribution.

High purity fittings and tubing.

1/8" Bubbler legs in and out of each source.

Uniframe™ Growth Cabinet (12') consisting of a 12' Steel growth cabinet (includes space for growth chamber, loadlock, gas panel, refrigerator baths, vacuum system and electronics), built-in light, Interlocked clear lexan soft-seal doors and solid panel soft-seal doors.

Lauda Liquid Refrigeration Bath

TMGa Standard Source Manifold

TEGa Standard Source Manifold

TMAI Standard Source Manifold

TMIn Dual Bubbler Standard Source Manifold

Cp2Mg Single Bubbler Standard Source Manifold

SiH4 Single Input with Dilution Manifold

NH3 Single Input Hydride Manifold

System Electronics and Control Modules –

EMCORE™ standard control modules for Substrate Rotation, Reactor Temperature Control, Reactor Pressure, System Logic Control, and Pump Activation.

Integrated power load center with Emergency Power Off switch.

+15, -15, +24 VDC Power Supplies.

Microprocessor unit with analog and digital control boards, input boards, and RS232/Ethernet ports for communication.

EpiView™ Control and Monitoring System

EpiView™ Control and Monitoring Software.

Graphical display windows for all gas panel, growth chamber, and exhaust components.

User-configurable parameters for valve states, analog scales and set points.

Data logging and viewing with configurable data rate and signal selection.

Export of data files to Microsoft Excel for analysis and presentation, with automatic data compression.

Advanced troubleshooting and diagnostic tools, automated maintenance.

Report generator for run analysis.

Event recording of system status and alarms.

Definable levels for system security.

EpiView Industrial PC System

Industrial Based Modular PC (Pentium III 1 GHz)

High Resolution LCD Monitor, 16 MB Video Card.

2 Network Cards enabling PC-System and PC-Facility connection.

Microsoft® Windows 2000, Service Pack with Microsoft® Word and Excel '2000.

Hydrogen Detector

Aeronex Gatekeeper™ 500K NH3 Purifier

Nickel Metallic purifying media.

Outlet purity <1 ppb contaminants (H2O, O2).

Integrated 0.003 micron particle filter.

Isolation valves on inlet & outlet.

Aeronex Gatekeeper™ 500K H2 Purifier

Nickel Metallic purifying media.

Outlet purity <1 ppb contaminants (H2O, O2).

Integrated 0.003 micron particle filter.

Isolation valves on inlet & outlet.

Aeronex Gatekeeper™ 500K N2 Purifier

Nickel Metallic purifying media.

Outlet purity <1 ppb contaminants (H2O, O2).

Integrated 0.003 micron particle filter.

Isolation valves on inlet & outlet.

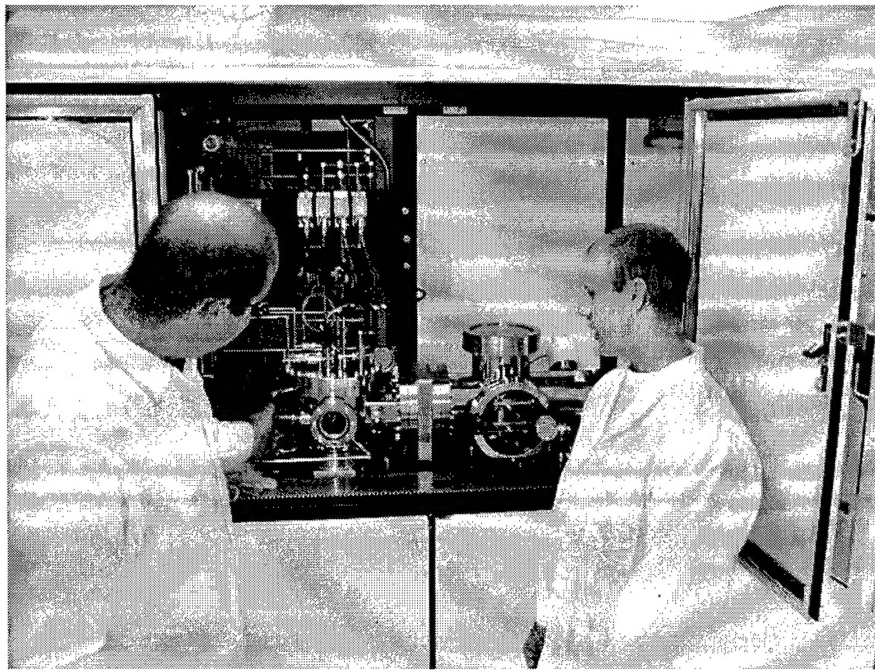


Fig. 1. Jerry Thaler, Post-Doc, and Mark Hlad, graduate student, observing the sample transfer process in the Veeco P75 MOCVD reactor at the new University of Florida GaN epitaxial facility.

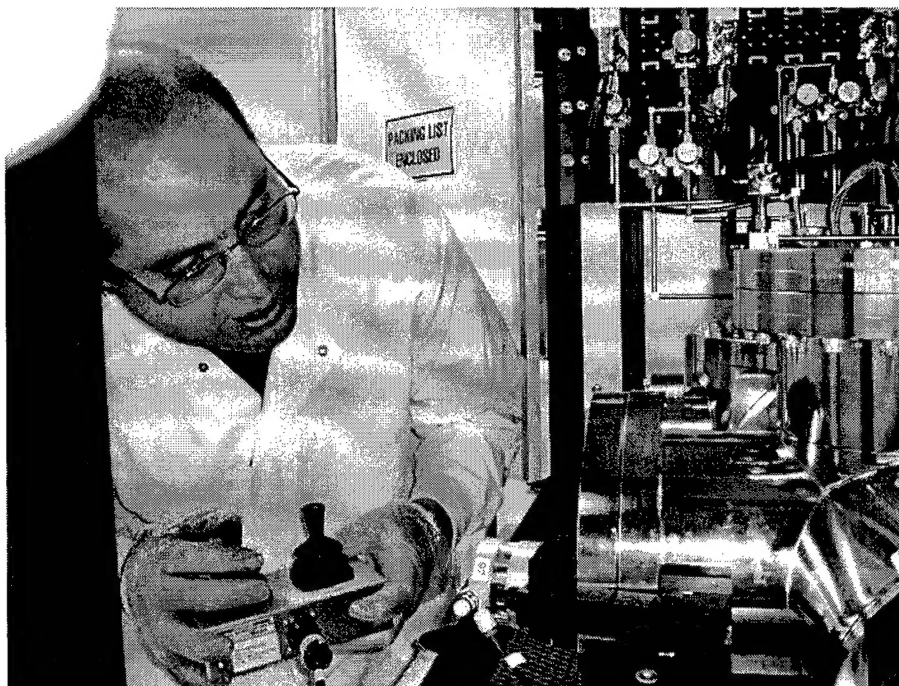


Figure 2. Jerry Thaler, Post-Doc, manipulating a sample in the growth chamber of the Veeco P75 MOCVD reactor at UF.

In addition to the reactor itself, ancillary equipment including a fully automated gas cabinet and a point of use BOC scrubber were also installed in this lab, shown in Figure 3. These items were obtained through a combination of industrial donation and UF funds. This new facility also includes a dual exhaust wet chemical hood to allow for pre and post-growth sample preparation and handling, shown in Figure 4. Extensive renovation of the laboratory was required prior to installation of the MOCVD reactor, and was paid for by the university. Final installation is almost complete with facility sign off by the UF Environmental Health and Safety Department expected this week.

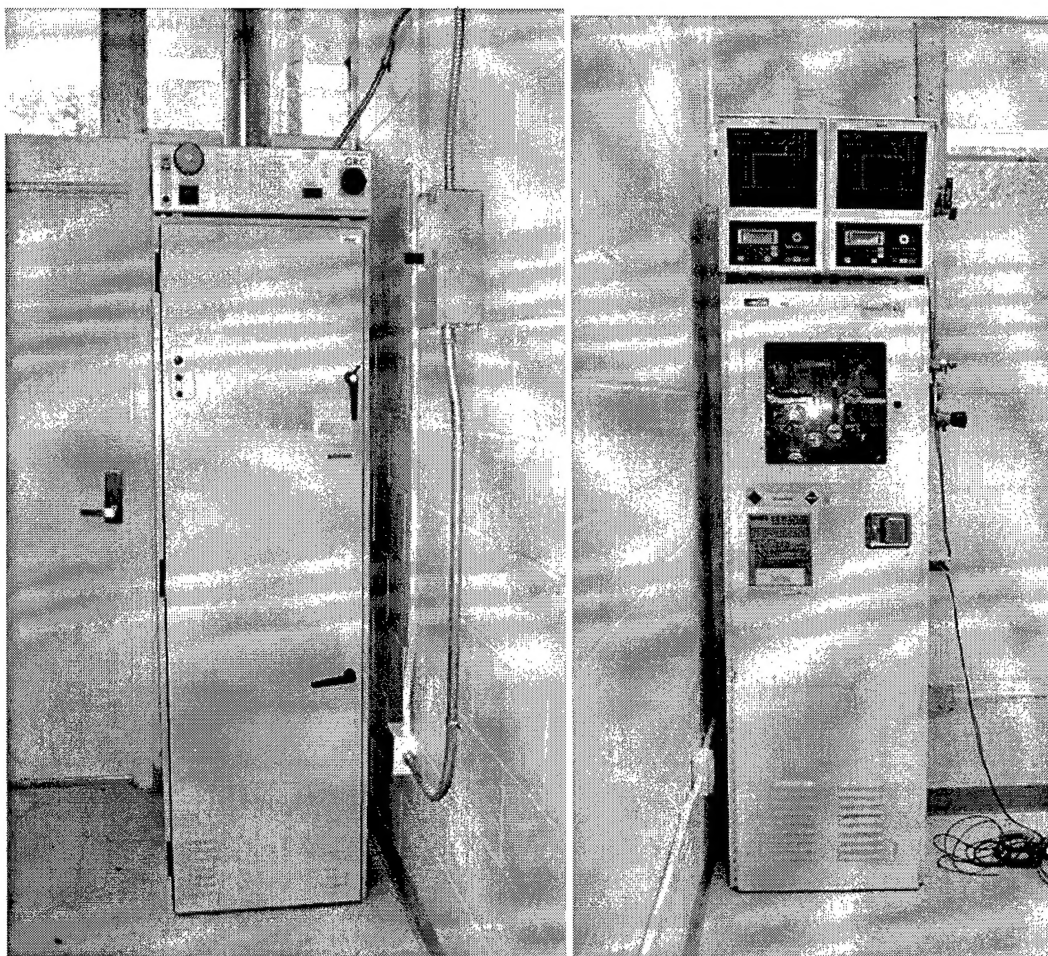


Figure 3. BOC scrubber, at left, and Air Products gas cabinet, at right, installed in the UF GaN MOCVD facility.

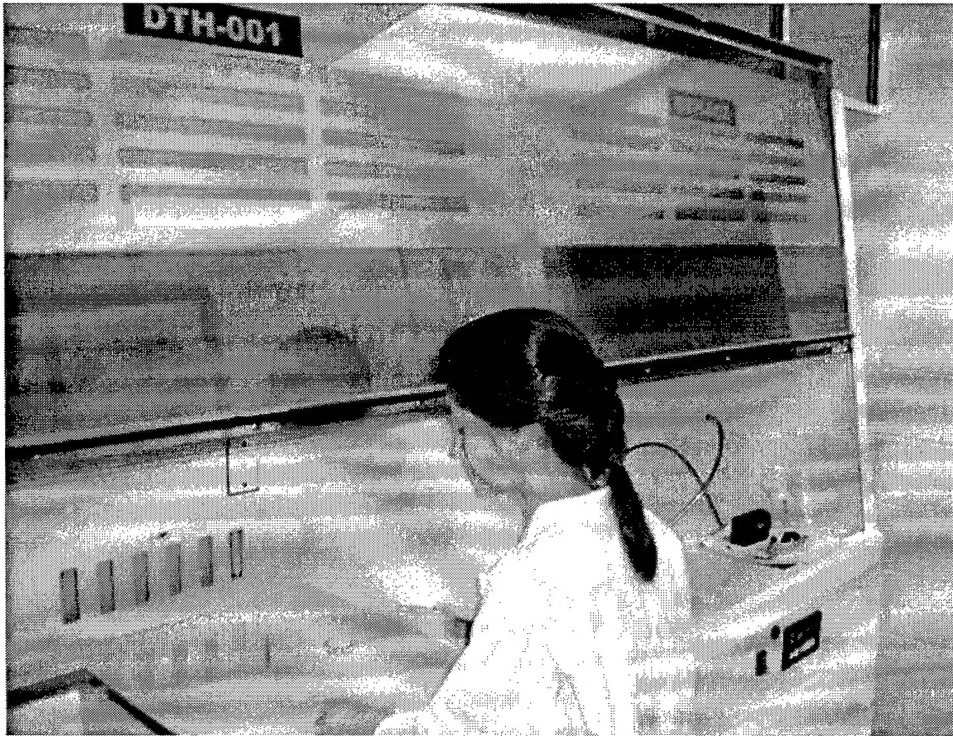


Figure 4. Jennifer Hite, graduate student, preparing substrates in the wet chemical hood in the new University of Florida GaN epitaxial facility.

4. References

1. N. X. Nguyen, M. Micovic, W.-S. Wong, P. Hashimoto, L.-M. McCray, P. Janke, C. Nguyen, *Electron. Lett.* **36**, 468(2000).
2. Y. -F. Wu, B. P. Keller, S. Keller, D. Kapolnek, P. Kozodoy, S. P. DenBaars and U. K. Mishra, *Solid-State Electron.*, **41**, 1569(1997).
3. M. A. Khan, X. Hu, G. Simin, A. Lunev, J. Yang, R. Gaska, and M.S. Shur, *IEEE Electron. Dev. Lett.* **21**, 63(2000).
4. K. K. Chu, J. A. Smart, J. R. Shealy and L. F. Eastman, Proc. State-of-The-Art Program on Compound Semiconductors (SOTAPOCS XX/X, Electrochem. Soc., Pennington, NJ 1998), M.3-12.
5. B. M. Green, K. K. Chu, E. M. Chumbes, J. A. Smart, J. R. Shealy, and L. F. Eastman, *IEEE Electron. Dev. Lett.*, **21**, 268(2000).
6. S. C. Binari, W. Kruppa, H. B. Dietrich, G. Kelner, A. E. Wickenden and J. A. Freitas Jr, *Solid-State Electron.*, **41**, 1549(1997).
7. L. F. Eastman, V. Tilak, J. Smart, B. M. Green, E. M. Chumbes, R. Dimitrov, H. Kim; O. S. Ambacher, N. Weimann, T. Prunty, M. Murphy, W. J. Schaff, and J. R. Shealy, *IEEE Trans. Electron Dev.*, **48**, 479(2001).
8. Y. -F. Wu, B. P. Keller, S. Keller, D. Kapolnek, P. Kozodoy, S. P. DenBaars and U. K. Mishra, *Solid-State Electron.*, **41**, 1569(1997).

9. J. W. Johnson, A.G. Baca, R. D. Briggs, R. J. Shul, C. Monier, F. Ren, S. J. Pearton, A. M. Dabiran, A. M. Wowchack, C. J. Polley and P. P. Chow, *Solid-State Electron.*, **45**, 1979(2001).
10. W. Lu, J. Yang, M. A. Khan and I. Adesida, *IEEE Trans. Electron Dev.*, **ED48**, 581(2001).
11. S. J. Pearton, J. C. Zolper, R. J. Shul and F. Ren, *J. Appl. Phys.*, **86**, 1(1999).
12. M. Asif Khan, Q. Chen, Michael S. Shur, B. T. Dermott, J. A. Higgins, J. Burm, W. J. Schaff and L. F. Eastman, *Solid-State Electron.*, **41**, 1555(1997).
13. G. Simin, X. Hu, N. Ilinskaya, A. Kumar, A. Koudymov, J. Zhang, M. Asif Khan, R. Gaska, M. S. Shur, *Electron. Lett.* **36**, 2043(2000).
14. E. Kohn, I. Daumiller, P. Schmid, N. X. Nguyen, C. N. Nguyen, *Electron. Lett.* **35**, 1022(1999).
15. J.-S. Lee; A. Vescan, A. Wieszt, R. Dietrich, H. Leier, Y.-S. Kwon, *Electron. Lett.* **37**, 130(2001).
16. X. Hu, A. Koudymov, G. Simin, J. Yang, M. Asif Khan, A. Tarakji, M. S. Shur, and R. Gaska, *Appl. Phys. Lett.* **79**, 2832(2001).
17. N. X. Nguyen, C. Nguyen and D. E. Grider, *Electron. Lett.* **35**, 1356(1999).
18. I. Daumiller, C. Kirchner, M. Kamp, K. J. Ebeling, and E. Kohn, *IEEE Electron. Dev. Lett.* **20**, 448(1999).
19. A. Tarakji, G. Simin, N. Ilinskaya, X. Hu, A. Kumar, A. Koudymov, J. Yang, M. Asif Khan, M. S. Shur, and R. Gaska, *Appl. Phys. Lett.* **78**, 2169(2001).
20. E. M. Chumbes, J. A. Smart, T. Prunty and J. M. Shealy, *IEEE Trans. Electron Dev.*, **48**, 416(2001).
21. B. Luo, J. W. Johnson, F. Ren, K. K. Allums, C. R. Abernathy, S. J. Pearton, R. Dwivedi, T. N. Fogarty, R. Wilkins, A. M. Dabiran, A. M. Wowchack, C. J. Polley, P. P. Chow and A. G. Baca, *Appl. Phys. Lett.*, **79**, 2196(2001).
22. S. J. Pearton, F. Ren, A. P. Zhang and K. P. Lee, *Mat. Sci. Eng. Rep. R30*, 55(2000).
23. S. C. Binari, K. Ikossi, J. A. Roussos, W. Kruppa, D. Park; H. B. Dietrich, D. D. Koleske, A. E. Wickenden, and R. L. Henry, *IEEE Trans. Electron Dev.*, **48**, 465(2001).
24. G. Soc. G303(2001).
25. M. S. Shur, Solid Simin, A. Koudymov, A. Tarakji, X. Hu, J. Yang, M. Asif Khan, M. S. Shur, and R. Gaska, *Appl. Phys. Lett.* **79**, 2651(2001).
26. F. Ren, M. Hong, S. N. G. Chu, M. A. Marcus, M. J. Schurman, A. Baca, S. J. Pearton, and C. R. Abernathy, *Appl. Phys. Lett.*, **73**, 3893(1998).
27. J. W. Johnson, B. Luo, F. Ren, B. P. Gila, V. Krishnamoorthy, C. R. Abernathy, S. J. Pearton, J. I. Chyi, T. E. Nee, C. M. Lee, and C. C. Chuo, *Appl. Phys. Lett.*, **77**, 3230(2000).
28. B. P. Gila, J. W. Johnson, K. N. Lee, V. Krishnamoorthy, C. R. Abernathy, F. Ren, and S. J. Pearton, *ECS Proc. Vol.*, **2001-1**, 71(2001).
29. M. Asif Khan, X. Hu, A. Tarakji, G. Simin, J. Yang, R. Gaska, and M. S. Shur, *Appl. Phys. Lett.* **77**, 1339(2001).
30. G. Simin, X. Hu, N. Ilinskaya, J. Zhang, A. Tarakji, A. Kumar, J. Yang, M. Asif Khan, R. Gaska, M. S. Shur, *IEEE Electron. Dev. Lett.* **22**, 53(2001).
31. J. W. Johnson, B. P. Gila, B. Luo, K. P. Lee, C. R. Abernathy, S. J. Pearton, J. I. Chyi, T. E. Nee, C. M. Lee, C. Chou and F. Ren, *J. Electrochem. -State Electron.* **42**, 2131(1998).
32. Hadis Morkoç, Aldo Di Carlo and Roberto Cingolani, *Solid-State Electron.* **46**, 157(2002).
33. Y. Ohno, M. Kuzuhara, *IEEE Trans. Electron Dev.* **ED48**, 517(2001).

34. Y.-F. Wu; D. Kapolnek, J. P. Ibbetson, P. Parikh, B. P. Keller, U. K. Mishra, *IEEE Trans. Electron Dev.* **ED48**, 586(2001).
35. H. Morkoc, Nitride Semiconductors and Devices (Springer, Berlin, 1999).

REPORT DOCUMENTATION PAGE (SF298)
(Continuation Sheet)

Equipment Description and Budget Description

Pulsed-laser deposition is one of the most versatile and controllable techniques available for the growth of epitaxial metal oxide thin-film materials. In this film growth technique, a focused laser pulse is directed onto a target of material in a vacuum chamber. The laser pulse locally heats and vaporizes the target surface, producing an ejected plasma or plume of atoms, ions, and molecules. The plume of material is deposited onto an adjacent substrate to produce a crystalline film. This technique possesses several favorable characteristics for growth of multicomponent oxides, such as stoichiometric transfer of target material to the substrate, compatibility with a background oxygen gas, and atomic level control of the deposition rate. In order to fully exploit the capabilities of this technique in controlling oxide film growth at the atomic level, one should be able to achieve and characterize atomically-defined surfaces during nucleation and film growth. This is possible under MBE-like UHV conditions. Laser molecular beam epitaxy (L-MBE) is a method for the atomic layer-by-layer growth of thin films in an MBE-like environment in which laser ablation targets serve as the source materials. L-MBE offers the control of film growth normally attributed to MBE, but with a significantly greater operating background pressure range, as laser ablation can effectively deposit films at pressures from UHV to 500 mTorr. It offers sub-monolayer digital control of the deposition process, and is particularly effective in the growth of complex oxide materials with molecular oxygen, atomic oxygen, or ozone as the oxidizing specie. In addition, laser ablation is effective at providing a growth flux of low vapor pressure components (e.g. ZrO_2 , HfO_2).

A laser molecular beam epitaxy system consists of a pulsed-laser deposition apparatus with an operating pressure ranging from several hundred mTorr to ultra high vacuum, reflection high energy electron diffraction for atomic-level characterization and control of surface properties and nucleation, an excimer laser for laser ablation of source targets, beam-handling optics and excimer gas source. Thermionics Laboratory, Inc currently markets a commercial laser-MBE system that was originally designed by the PI while serving as a research staff member at Oak Ridge National Laboratory. Two systems have been in service at ORNL for over four years. With routine maintenance, this equipment will be useful in excess of ten years. In addition, the chamber design will be modified so as to accommodate high-pressure reflection high-energy electron diffraction as well as the future addition of other surface analytical capabilities via UHV sample transfer. An excimer laser is current available at the University of Florida for use with this system. The equipment cost for the UHV pulsed-laser deposition system equipped with reflection high energy electron diffraction capabilities was approximately \$300,000, and involved major purchases from various vendors including Thermionics, Staib, and Pumpworks.

DOD-Related Research in Complex Oxides

The diverse functionality of complex oxides lends itself to a large array of thin-film applications that directly impact defense-related technologies. Paraelectric films with voltage-dependent dielectric properties can be used as tunable microwave components for wireless communication or radar systems. High-k dielectric and ferroelectric oxides on semiconductors are actively being considered to replace SiO_2 as the gate dielectric in next-generation MOSFET devices. Luminescent oxide thin films are potentially applicable for either cathodoluminescent or electroluminescent flat-panel display technologies. The development of planar thin-film waveguide components could prove enabling in the integration of high-speed optical communication systems. In addition, current efforts to develop magnetic spin-based electronics include the study of conducting and semiconducting magnetic oxide thin-film materials. In all cases, control of oxide interface properties and defect densities afforded by atomic-level control of epitaxy will be necessary in order to implement these novel technology concepts. In addition, nanoscale understanding and manipulation of material properties present real possibilities in improving material performance and/or developing *new* device concepts that could revolutionize

communication and computing technologies. In order to lend specificity to the planned use of the requested L-MBE system anticipated projects are described in detail below.

i. Fundamental Properties of Tunable Ferroelectric/Paraelectric Materials

In high frequency applications, ferroelectric films are currently being considered as the dielectric medium in tunable capacitors for development of phase-shifting elements for beam steering and of low phase noise voltage controlled oscillators for high frequency applications. In designing materials for these applications, it is advantageous to tune the composition such that the material is marginally in the paraelectric state at the operating temperature. This eliminates losses due to ferroelectric domain wall motion. One of the most attractive material systems for both understanding and manipulating ferroelectric/paraelectric properties is $\text{K}(\text{Nb,Ta})\text{O}_3$. It is similar to $(\text{Sr,Ba})\text{TiO}_3$ in that the solid solution possesses a continuous transition from a paraelectric to a ferroelectric material. KTaO_3 is cubic ($a_{300} = 3.9885 \text{ \AA}$) and paraelectric at all temperatures. Decreasing temperature results in a softening of the TO_1 transverse optic zone center phonon branch. As the soft mode is stabilized by zero-point quantum fluctuations, KTaO_3 does not undergo a ferroelectric transition but remains cubic and paraelectric down to 0 K, hence it is generally believed to be an incipient ferroelectric. KNbO_3 , in contrast, exhibits a first-order ferroelectric phase transition accompanied by a change from the cubic to the tetragonal structure at 701 K ($a_p = 4.02 \text{ \AA}$ along $[100]_p$ and $[010]_p$ directions, and $c_p = 3.97 \text{ \AA}$ along the $[001]_p$). Upon further cooling, the structure changes to orthorhombic at 498 K, with lattice parameters $a = 5.696 \text{ \AA}$, $b = 5.7213 \text{ \AA}$, and $c = 3.9739 \text{ \AA}$. For the ferroelectric state, the polarization direction is along the $[010]$ (b axis). It is important to note that cubic KTaO_3 is well lattice matched to the cubic and tetragonal KNbO_3 , as the pseudo-cubic lattice parameter of KNbO_3 ($a_p = 4.014 \text{ \AA}$, $T = 25^\circ\text{C}$) differs from that for KTaO_3 by only 0.6 %.

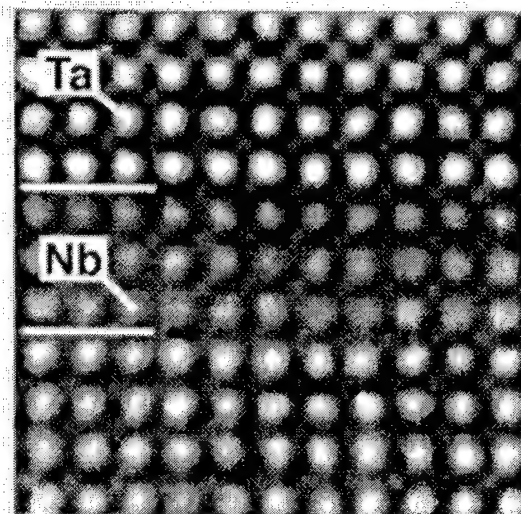
As a solid solution, the Curie temperature varies continuously according to the formula $T_c = 676x + 32$ (for $x > 4.7\%$). For $x > 0.35$, the solid solution exhibits a first-order ferroelectric phase transition similar to KNbO_3 . The ferroelectric transition is characterized by the appearance of a remnant polarization that is due to off-center Nb and Ta ions. For $x < 0.35$, dielectric and polarization measurements suggest a diffuse character for the ferroelectric transition. Evidence suggests that the transition in this region takes place in two steps: first, a progressive appearance of polar cells around single or groups of Nb ions occurs; second, the collective ordering of the individual electric dipoles occurs due to mutual strain between cells. There are also indications that fluctuations of mesoscopic scale ferroelectric domains contribute to the dielectric response.

At or near the Curie temperature, electric field-induced changes in the dielectric constant on the order of 80% have been observed in bulk $\text{K}(\text{Ta,Nb})\text{O}_3$. Due to its low dielectric loss, high saturation polarization, large electrooptic effects, and low driving voltage for modulation, $\text{KTa}_{1-x}\text{Nb}_x\text{O}_3$ is also an attractive material for applications involving holographic data storage, parametric oscillators, pyroelectric detectors, and second harmonic generators. $\text{K}(\text{Ta,Nb})\text{O}_3$ thin films have been realized using a variety of techniques, including sputtering, sol-gel, liquid-phase epitaxy and pulsed-laser deposition. Recent developments in oxide film growth provide the opportunity to understand, control, and manipulate the growth of epitaxial oxide films and multilayers at the atomic scale. Unfortunately, relatively little work has been reported on the atomic layer-by-layer growth of $\text{K}(\text{Nb,Ta})\text{O}_3$ thin films when compared to the effort on the $(\text{Ba,Sr})\text{TiO}_3$ system. One difficulty in synthesizing high quality $\text{K}(\text{Nb,Ta})\text{O}_3$ thin films relates to the high volatility of K. However, recent efforts have circumvented this problem by providing an excess K flux during epitaxy.

ii. Reduced Dimensionality in Ferroelectrics and Dielectrics

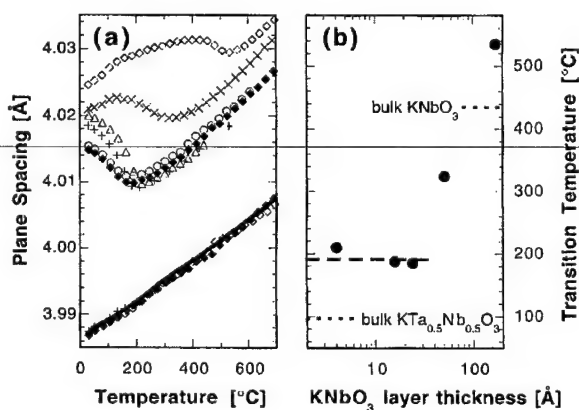
Finite size effects in ferroelectrics have been a subject of study for several years, although most studies have focused on small particle size in ceramic materials as opposed to epitaxial thin films. Using the Landau-Devonshire theory, Zhong et al. have shown that the ferroelectric transition temperature is expected to decrease with decreasing size, resulting in a size-driven transition from ferroelectric to paraelectric behavior. Recently, the effects of nanostructure and dimensionality on ferroelectricity in KNbO_3 have been explored. $\text{K}(\text{Nb,Ta})\text{O}_3$ thin films and $\text{KNbO}_3 / \text{KTaO}_3$ superlattices have been grown by pulsed laser deposition on KTaO_3 (001) substrates. Excellent film flatness and crystallinity are evidenced in these films, and the interfaces are found to

be compositionally sharp on an atomic scale. Unlike $(\text{Sr,Ba})\text{TiO}_3$, the $\text{K}(\text{Nb,Ta})\text{O}_3$ system displays very little change in the average d-spacing in moving across the alloy composition. This significantly minimizes the effects of strain in superlattices, and enables the synthesis of commensurate structures with low defect density. Symmetric superlattice structures consisting of alternating atomic-scale layers of KTaO_3 and KNbO_3 with variable periodicity have been fabricated and studied. While relatively thick KNbO_3 films are characterized by an orthorhombic structure, the $\text{KTaO}_3 / \text{KNbO}_3$ superlattices are uniformly strained in-plane without misfit dislocations, imposing an in-plane KNbO_3 lattice spacing that is identical to that of the KTaO_3 substrate. A tetragonal-to-tetragonal transition was observed in which the phase transition temperature, T_c , determined by temperature-dependent x-ray diffraction, depends on the KNbO_3 layer thickness. The in-plane strain also results in a significant increase in this ferroelectric-paraelectric T_c for superlattices relative to thick KNbO_3 layers and random alloy films. As the superlattice period decreases, a reduction of T_c is observed. For symmetric superlattices with periodicities of 50 Å or less, the Curie temperature is identical to that of the $\text{K}(\text{Ta}_{0.5}\text{Nb}_{0.5})\text{O}_3$ random alloy film, indicating significant long-range ferroelectric coupling across the KTaO_3 layers.



Z-contrast STEM image of $\text{KTaO}_3/\text{KNbO}_3$ superlattice grown by pulsed laser deposition, showing the atomically-abrupt interface between adjacent layers.

These initial results from studies of symmetric $\text{KTaO}_3 / \text{KNbO}_3$ superlattices present a number of interesting questions and opportunities, particularly with regard to nanoscale modification of dielectric properties. For example, it is not clear whether the ferroelectric phase transition is sharp (first order) or diffuse when T_c is shifted by a combination of finite size and strain effects in superlattice structures. The imposed inhomogeneity in the layered structures should affect the nature of the transition, particularly if it is primarily driven by next nearest neighbor interactions.

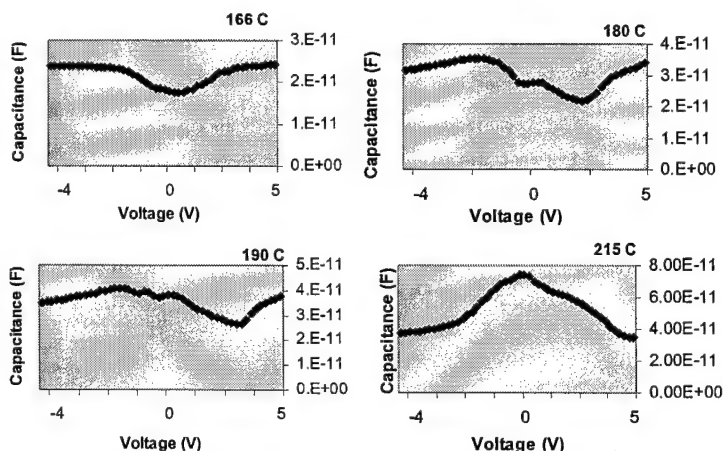


Transition temperature as a function of KNbO_3 thickness for symmetric $\text{KTaO}_3/\text{KNbO}_3$ superlattices.

the capacitance with an applied dc bias voltage.

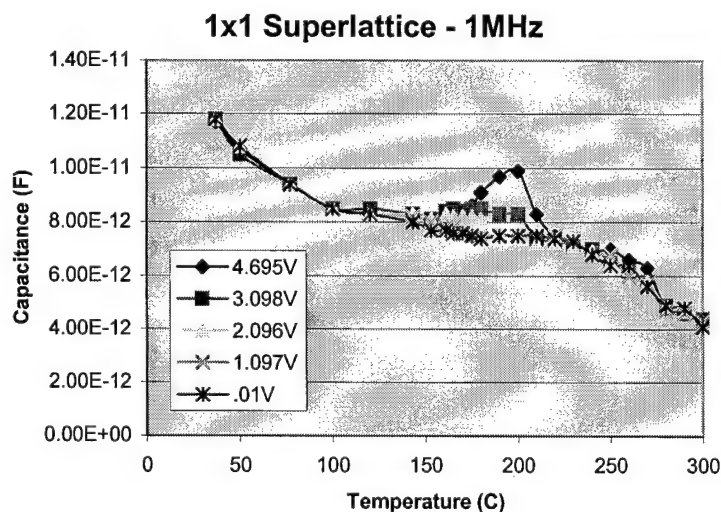
Recently, we initiated a study of the temperature-dependent dielectric response in these symmetric superlattice structures, with specific interest in the behavior near the apparent phase transition observed in the X-ray diffraction results cited earlier. In particular, the dielectric response of 1 unit cell x 1 unit cell (1x1) $\text{KTaO}_3 / \text{KNbO}_3$ superlattices and $\text{K}(\text{Ta}_{0.5}\text{Nb}_{0.5})\text{O}_3$ alloy films were studied at 100 kHz and 1 MHz by measuring the capacitance of interdigitated electrodes deposited on the surfaces. Electrode finger separation and width were both 10 μm . Each capacitor structure consisted of 26 fingers. The capacitance was measured as a function of temperature from 25 to 275 $^{\circ}\text{C}$. The structural phase transition temperature seen in the previous X-ray diffraction data was located at approximately 200 $^{\circ}\text{C}$. Voltage tunability was also measured over this temperature range by measuring

The temperature-dependent capacitance for a (1x1) $\text{KTaO}_3 / \text{KNbO}_3$ superlattice measured at 100 kHz exhibits interesting behavior, particularly in terms of the bias voltage dependence. For temperatures less than approximately 130°C , the capacitance is nearly temperature independent with almost no discernable bias voltage dependence. From the previous X-ray diffraction results and phase behavior for $\text{K}(\text{Nb,Ta})\text{O}_3$, we expected the film to be ferroelectric in this temperature regime. Increasing the temperature above 130°C results in an increase in the dielectric response. In addition, anomalous positive dc voltage dependence in the capacitance is observed. In particular, the capacitance is seen to increase with applied dc bias. This positive tunability is clearly seen in capacitance versus voltage plots. This type of nonlinear dielectric behavior is unusual and not typically observed in $\text{K}(\text{Ta,Nb})\text{O}_3$ thin films. A maximum in the positive dc bias tunability is observed at approximately 175°C . For temperatures greater than 190°C , a crossover is observed where the tunability becomes negative as is normally seen in paraelectric thin films. Note that this is also the same temperature range where a phase transition is observed in the temperature-dependent X-ray diffraction data. At approximately 230°C , the tunability is greater than 50% with an applied voltage of only 4.7 V. The transition from positive to negative tunability is clearly observed. It should also be noted that, while the capacitance steadily increases as the temperature increases up to 240°C , there is a local maximum observed in the capacitance at approximately 205°C . Again, this roughly corresponds to the structural phase transition observed for the same sample using X-ray diffraction. Temperature-dependent capacitance was also measured at 1 MHz for the same 1x1 $\text{KTaO}_3 / \text{KNbO}_3$ superlattice sample. Again, a large positive tunability is observed, although for 1 MHz it is pronounced only at the temperature corresponding to the structural phase transition. While the zero bias capacitance curve shows no identifiable structure suggesting a phase transition, the biased curves clearly show evidence for a transition at 195°C .



Capacitance behavior in 1x1 $\text{KTaO}_3/\text{KNbO}_3$ superlattices, measured as a function of dc bias voltage, shows an anomalous positive tunability at temperatures just below that corresponding to the structural transition.

Similar measurements were performed on $\text{K}(\text{Ta}_{0.5}\text{Nb}_{0.5})\text{O}_3$ alloy films. The alloy film does not exhibit this anomalous tunability behavior. Changes in the slope of the temperature-dependent capacitance are observed at 190°C , corresponding to the alloy structural phase transition. Since the average film composition is the same in both the alloy and superlattice film, the difference in the tunability behavior must be associated with the artificial ordering. More studies are needed in order to determine the origin of this behavior.



Anomalous positive tunability in capacitance is observed in $\text{KTaO}_3/\text{KNbO}_3$ superlattice structures.

Additional issues arise when one considers finite size effects in both the KNbO_3 and KTaO_3 layers. In previous studies, only symmetric super-lattices were considered. Changes in T_c reflected low dimensional effects in both layers.

Varying the KTaO_3 layer thickness while maintaining the KNbO_3 layer thickness allows one to directly probe the mechanisms for ferroelectric coupling across the paraelectric layer. In addition, one could examine whether the ferroelectric properties become anisotropic in either symmetric or asymmetric superlattices. From a fundamental point of view, it is important to understand whether the shift in T_c is due to finite size effects driven by electronic or phonon-related mechanisms. One could compare the properties of $\text{KTaO}_3/\text{KNbO}_3$ superlattices with structures in which the KTaO_3 layers are doped to yield semiconducting behavior. The carriers would screen electric fields and tend to decouple any electronic interactions that may participate. There is also a need to better understand the role of strain in determining phase transitions. Ferroelectric transitions are cooperative phenomenon in which both local dipole behavior and collective strain-related processes determine the material properties. The effects of reduced dimensionality need to be understood, and a delineation must be made between extrinsic (defect-related) and intrinsic properties of thin films. Superlattice structures allow the opportunity to impose a specific strain state on the layers, and may provide insight into its role in determining losses and tunability. One could also fabricate superlattices in which $\text{K}(\text{Ta},\text{Nb})\text{O}_3$ layers are embedded in a low-loss medium, such as MgAl_2O_4 , to observe the progressive suppression of loss and tunability as the $\text{K}(\text{Ta},\text{Nb})\text{O}_3$ volume fraction is decreased. The dielectric loss and tunability behavior in any of these $\text{K}(\text{Nb},\text{Ta})\text{O}_3$ -related superlattice structures has yet to be systematically studied..

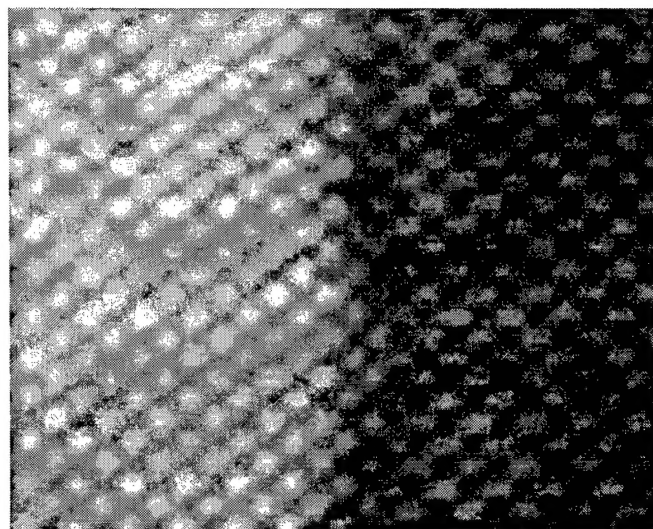
Perhaps one of the most challenging experiments to consider would be to compare these conventional superlattice structures possessing chemical modulation along the surface normal with superlattices in which the Ta/Nb modulation is along the in-plane direction. The formation of so-called, "lateral superlattices" represents a difficult challenge requiring an atomic-level control of the film growth based upon edge-mediated growth at atomic steps on the substrate surface. For these structures, the restrained lattice spacing would be along the chemical modulation direction (in-plane), and any ferroelectric transition would presumably involve a displacement parallel to the $\text{KTaO}_3/\text{KNbO}_3$ layer interfaces. With lateral superlattices, the possibility exists to locally probe the ferroelectric properties across the $\text{KTaO}_3/\text{KNbO}_3$ interface.

The issues discussed above are currently being investigated by the PI (D.P. Norton) through an Army Research Office research grant (DAAD 19-01-1-0508). The laser-MBE will be used to facilitate the synthesis and characterization of low-dimensional $\text{K}(\text{Nb},\text{Ta})\text{O}_3$ thin film structures. This equipment is necessary to perform three key activities within this project. First, we will investigate the nucleation and epitaxial growth of $\text{K}(\text{Nb},\text{Ta})\text{O}_3$ thin films at the atomic level so as to minimize defects that obscure the intrinsic effects of reduced dimensionality in these materials. This will include identifying conditions by which growth proceeds via island, layer-by-layer, or step flow. In conjunction with this study, we will investigate the synthesis of various 2- and 1-dimensional $\text{K}(\text{Nb},\text{Ta})\text{O}_3$ structures, including lateral superlattices and quantum wires fabricate-d in the step flow growth regime. In previous work, atomically ordered $\text{KNbO}_3 / \text{KTaO}_3$ superlattices have been shown to exhibit sharp structural transitions and unusual coupling as the KTaO_3 layer thickness is reduced. This research is directed at understanding and manipulating the nucleation and epitaxial growth of $\text{K}(\text{Ta},\text{Nb})\text{O}_3$ so as to enable the formation of well-defined interfaces and epitaxy-mediated cation ordering. Emphasis will be placed on controlling both dimensionality and interface boundary conditions in low defect epitaxial films. Thirdly, the macroscopic to nanoscale properties of these structures will be probed, with emphasis on understanding the effects of reduced dimensionality and interface boundary conditions on the ferroelectric phase transition and dielectric properties. This entails understanding the role of strain, finite size, and defect structures in determining the permittivity, loss tangent, tunability, and phase transitions in epitaxial thin films and superlattices. Specific emphasis will be given to delineating intrinsic from extrinsic mechanisms responsible for dielectric loss and tunability for paraelectric compositions. In collaboration with Mark Reeves at George Washington University, low and high frequency measurements, including non-contact microwave microscopy, will be used to characterize the dielectric properties. Capabilities include measurement of the electrical response at 1.7 GHz at length scales of 100 nm. This allows for the detection of defects on a microscopic scale and simultaneous correlation of topographic and electric features in the materials being measured. This research will significantly advance the understanding of epitaxial growth, nanostructure formation, and microscopic ferroelectric/paraelectric physical phenomenon in perovskite thin-film systems. The technical monitor for the current DOD-funded project is Dr. John Prater of the Army Research Office.

iii. Complex Oxides in Microelectronics

The integration of complex oxides on semiconductor platforms offers enabling opportunities in microelectronics. Future metal-oxide-semiconductor field-effect transistors (MOSFETs) will almost certainly incorporate high-k oxides as the gate dielectric. In addition, the growth of complex oxide films on semiconductors enables the integration of ferroic and luminescent functionality with digital electronics. In both cases, the atomic-scale properties of the oxide/semiconductor interface is key to device function. The epitaxial growth and properties of oxide thin films on dissimilar crystalline surfaces, such as semiconductors, offer significant challenges in both synthesis and property determination. In the growth of ionic oxide compounds on covalent, or near-covalent semiconductors, the properties of the interface are determined by both thermodynamic and kinetic influences. One must consider not only the usual issues of surface structure and lattice matching, but also the formation of competing oxide phases that are related to the native oxide of the semiconductor itself. In addition, one must also consider the stability of the interface once formed. All of these factors will influence the structural and electronic character of the oxide/semiconductor interface, and will determine the functionality of electronic oxide device structures on semiconductor platforms.

For several years, the investigator has studied the growth and properties of various electronic oxide thin-film materials, including dielectrics, ferroelectrics, phosphors, and superconductors. Included was an effort to understand the synthesis and properties of epitaxial electronic oxides on various semiconductor surfaces using pulsed-laser deposition and laser-molecular beam epitaxy. The latter approach involves the implementation of laser-ablation deposition in a UHV environment, thus enabling atomic-level control of the growth processes. Recent achievements include the development of a hydrogen-assisted PLD technique for epitaxy on semiconductor surfaces, resulting in the first heteroepitaxial growth of CeO_2 on (001) Ge for Ge MOSFET-type devices structures. In addition, L-MBE was used to achieve and alkaline earth silicide termination of (001) Si for perovskite epitaxy. Future work should focus on understanding the thermodynamics and kinetics of oxide epitaxy on semiconductors using RHEED. The interface properties need to be studied using complex impedance spectroscopy in order to correlate interface structure with electronic states. High-resolution Z-contrast STEM can then be used to determine the interfacial atomic structure. Future work will include understanding the fundamental properties of the CeO_2 /Ge interface, as well as the synthesis and properties of epitaxial oxide structures on various compound semiconductor surfaces, including III-V and II-VI compounds.



CeO_2

Ge

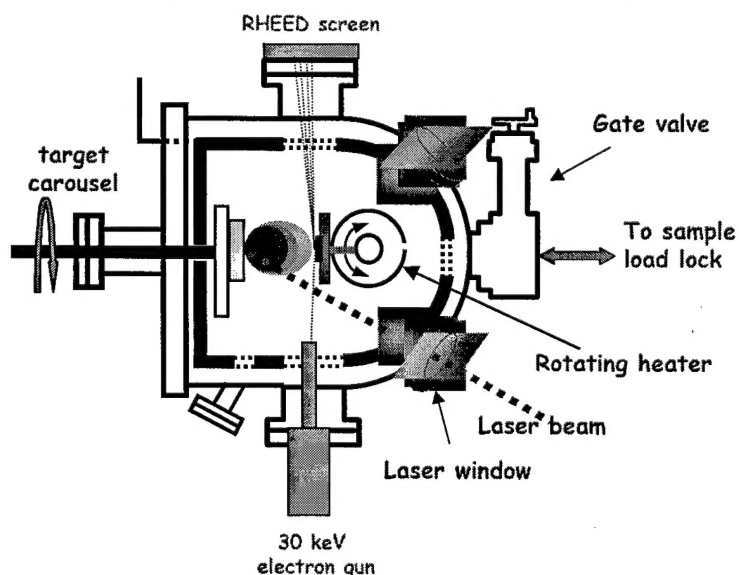
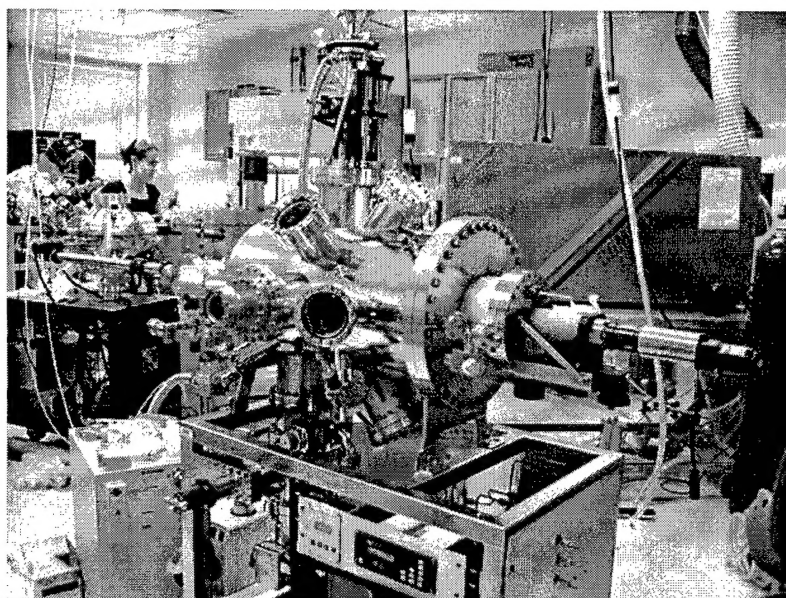
Z-STEM image of CeO_2 /Ge interface formed via L-MBE.

One of the more intriguing applications of complex oxides is as the active material in a junction-based or electric field-effect device. Although semiconducting oxides have long been used as chemical sensors, these materials have received little attention for other electronic applications due in large part to a relatively low carrier mobility. Nevertheless, the large energy bandgap makes these materials of potential use for several device concepts, including transparent electronics, light-emitting diodes, lasers, UV detectors, and high-temperature electronics. Recent theoretical arguments have also suggested that electric-field induced metal-insulator transitions in oxides that are Mott insulators could be useful for nanoscale digital switching. In addition to conventional charge-carrier devices, one could also consider the applicability of magnetically-doped

semiconducting oxides for so-called spintronic devices, in which the spin in a magnetic semiconductor is manipulated for switching. The recent discovery of ferromagnetic ordering in Mn-doped narrow band gap semiconductors has generated tremendous attention in this area. So far, the materials of interest have been the dilute magnetic semiconductors GaMnAs, InMnAs, and GaMnSb. Magnetism in oxides is relatively common; thus complex semiconducting oxides with magnetic impurities offer the opportunity to understand the coexistence of semiconducting and ferromagnetic properties.

Using L-MBE to control the synthesis of films and interfaces, we plan to investigate transport and doping in semiconducting oxides, focusing on the properties p - n junction and electric field-effect structures. Of particular interest will be i) Mott insulators, ii) dilute magnetic semiconducting, and ii) Zn-based oxides that possess a large energy gap with reasonably high conductivity and mobility due to a relatively low ionicity. This includes ZnO, which is a direct bandgap material with an energy gap comparable to GaN. One of the significant challenges in developing oxides for semiconductor applications is the need to achieve both p -type and n -type doping in the same oxide lattice.

The constructed LMBE system is shown in the figure below



Laser molecular beam epitaxy system constructed within this project.

List of equipment components:

UHV laser mbe chamber (Thermionics)	PO 488423	\$135,717.00
Vacuum pumps (pumpworks)	PO 500387	\$60,773.81
REED system (Staib Instruments)	PO v06182	\$56,090.00
Gas delivery system, chillers, optics	PO 488423	\$47,000.00
Newport Corporation (misc parts)	PO T95802	\$ 419.19

AWARD AMOUNT
FROM ARMY
230,000.00

University of Florida-Cost Sharing
Amount \$70,000.00

Total Cost of Performance
Amount \$300,000

MASTER COPY: PLEASE KEEP THIS "MEMORANDUM OF TRANSMITTAL" BLANK FOR REPRODUCTION PURPOSES. WHEN REPORTS ARE GENERATED UNDER THE ARO SPONSORSHIP, FORWARD A COMPLETED COPY OF THIS FORM WITH EACH REPORT SHIPMENT TO THE ARO. THIS WILL ASSURE PROPER IDENTIFICATION. NOT TO BE USED FOR INTERIM PROGRESS REPORTS; SEE PAGE 2 FOR INTERIM PROGRESS REPORT INSTRUCTIONS.

MEMORANDUM OF TRANSMITTAL

U.S. Army Research Office
ATTN: AMSRL-RO-BI (TR)
P.O. Box 12211
Research Triangle Park, NC 27709-2211

☐ Reprint (Orig + 2 copies)

☐ Technical Report (Orig + 2 copies)

☐ Manuscript (1 copy)

X Final Progress Report (Orig + 2 copies)

☐ Related Materials, Abstracts, Theses (1 copy)

CONTRACT/GRANT NUMBER: DAAD19-02-1-0166

REPORT TITLE: Final Report: "Laser Molecular Beam Epitaxy System for Nanostructured Oxides)

is forwarded for your information.

SUBMITTED FOR PUBLICATION TO (applicable only if report is manuscript):

Sincerely, David P. Norton, Professor